Atmos. Chem. Phys. Discuss., doi:10.5194/acp-2016-1107, 2017
Manuscript under review for journal Atmos. Chem. Phys.
Published: 25 January 2017


Atmospheric Chemistry and Physics Discussions

# Decoupling peroxyacetyl nitrate from ozone in Chinese outflows observed at Gosan Climate Observatory

**Jihyun Han[1*], Meehye Lee[1], Gangwoong Lee[2], Louisa K. Emmons[3]**

[1]Department of Earth and Environmental Sciences, Korea University, Seoul, Republic of Korea
[2]Department of Environmental Science, Hankuk University of Foreign Studies, Yongin, Republic of Korea
[3]Atmospheric Chemistry Observations and Modeling Laboratory, National Center for Atmospheric Research (NCAR), Boulder, CO, USA
*now at: Korea Environment Institute, Sejong, Republic of Korea

Correspondence to: M. Lee (meehye@korea.ac.kr )

Submitted to Atmospheric Chemistry and Physics

December 2016

Atmos. Chem. Phys. Discuss., doi:10.5194/acp-2016-1107, 2017
Manuscript under review for journal Atmos. Chem. Phys.
Published: 25 January 2017


Atmospheric Chemistry and Physics Discussions

**Abstract**

We measured peroxyacetyl nitrate (PAN) and other reactive species such as $O_3$, $NO_2$, CO, and $SO_2$ with aerosols including $PM_{10}$ and $PM_{2.5}$ organic carbon (OC) and elemental carbon (EC) at Gosan Climate Observatory in Korea (33.17°N, E126.10°E) during October 10 to November 6, 2010. PAN was determined through fast gas chromatography with luminol chemiluminescence detection at 425 nm every 2 min. The PAN mixing ratios ranged from 0.1 (detection limit) to 2.4 ppbv with a mean of 0.6 ppbv. For all measurements, PAN was unusually better correlated with $PM_{10}$ (Pearson correlation coefficient, $\gamma = 0.75$) than with $O_3$ ($\gamma = 0.67$). In particular, the $O_3$ level was highly elevated with $SO_2$ at midnight, along with a typical midday peak when air was transported rapidly from the Beijing areas. The PAN enhancement was most noticeable during the occurrence of haze under stagnant conditions. In Chinese outflows slowly transported over the Yellow Sea, PAN gradually increased up to 2.4 ppbv at night, in excellent correlation with a concentration increase of $PM_{2.5}$ OC and EC, $PM_{1.0}$ $K^+$, and $PM_{10}$ mass. The high $K^+$ and OC/EC ratio indicated that the air mass was impacted by biomass combustion. This study highlights PAN decoupling with $O_3$ in Chinese outflows and suggests PAN as a potential indicator of overall aerosol formation in aged air masses impacted by biomass burning.

Key words: PAN, $O_3$, $PM_{10}$, Chinese outflow, Haze, Biomass combustion

Atmos. Chem. Phys. Discuss., doi:10.5194/acp-2016-1107, 2017
Manuscript under review for journal Atmos. Chem. Phys.
Published: 25 January 2017


Atmospheric Chemistry and Physics Discussions

## 1. Introduction

At the surface, ozone is primarily photochemically produced, and the contribution from the stratosphere is generally small. Ozone is formed through reactions of various precursors such as CO, $CH_4$, volatile organic compounds (VOCs), and $NO_x$ (e.g., Brasseur et al., 1999; Jacob, 2000; Nielsen et al., 1981). Likewise, peroxyacetyl nitrate (PAN) is a secondary product of urban air pollution and a significant oxidant in the atmosphere (e.g., Hansel and Wisthaler, 2000; La Franchi et al., 2009; Lee et al., 2012; Liu et al., 2010; Roberts et al., 2007). PAN is solely produced by the photochemical reaction between the peroxyacetyl radical and nitrogen dioxide, and the peroxyacetyl radical is derived from the OH oxidation or photolysis of VOCs such as acetaldehyde, methylglyoxal, and acetone (e.g., Fischer et al., 2014; La Franchi et al., 2009; Lee et al., 2012). For this reason, PAN is a very useful indicator of photochemical air pollution. As thermal decomposition is a major PAN sink in the troposphere (Beine et al., 1997; Jacob, 2000; Kenley and Hendry, 1982; Talukdar et al., 1995), the lifetime of PAN depends on temperature. For example, the PAN lifetime is ~5 years at −26°C and 1 h at 20°C (Fischer et al., 2010; Zhang et al., 2011). At high altitudes above ~7 km, photolysis becomes the most important loss process for PAN (Talukdar, et al., 1995). Thus, PAN can be an indicator of $NO_y$ concentration in the free troposphere in urban areas and a guide for the long-range transport of $NO_x$ in remote regions (Jacob, 1999).

In the past decades, PAN was measured not only in urban areas (Aneja et al., 1999; Gaffney et al., 1999; Grosjean et al., 2002; Lee et al., 2008; Zhang et al., 2014) but also in background regions (Fischer et al., 2011; Kanaya et al., 2007; Lee et al., 2012), onboard aircraft (Tereszchuk et al., 2013), and ships (Roberts et al., 2007). PAN concentrations were in the range of a few ppbv in urban areas close to VOCs and $NO_x$ sources (Lee et al., 2008; Zhang et al., 2011). In remote regions, PAN mixing ratios were generally in the range of a

Atmos. Chem. Phys. Discuss., doi:10.5194/acp-2016-1107, 2017
Manuscript under review for journal Atmos. Chem. Phys.
Published: 25 January 2017




few pptv (Gallagher et al., 1990; Mills et al., 2007; Muller and Rudolph, 1992; Staudt et al., 2003).

In recent years, $NO_x$ and VOCs have gradually increased in East Asia, particularly China (Akimoto, 2003; Liu et al., 2010; Ohara et al., 2007), leading to an increase in the concentrations of photochemical byproducts such as PAN and $O_3$ not only in East Asia (Liu et al., 2010; Wang et al., 2010; Zhang et al., 2009; Zhang et al., 2011; Zhang et al., 2014) but also in North America (Fischer et al., 2010; Fischer et al., 2011; Jaffe et al., 2007; Zhang et al., 2008). These results were also demonstrated by the GEOS-Chem model (Zhang et al., 2008). In addition to urban plumes, PAN was reported to be enhanced by biomass combustion (Alvarado et al., 2010; Coheur et al., 2007), such as open burning and use of biofuel, which is used to take place often in China after crop harvesting (Cao et al., 2006; Duan et al., 2004). In this context, PAN is a useful indicator for diagnosing Chinese outflows and assessing their perturbation on regional air quality in the northwestern Pacific region.

Gosan Climate Observatory (GCO) is an ideal place to monitor Asian outflows and their transformation and to estimate their impact on air quality over the northern Pacific region (Lee et al., 2007; Lim et al., 2012). In the present study, PAN was first measured continuously at GCO to characterize its variation and source in relation to $O_3$ and to understand the influence of Chinese outflows on the regional air quality.

## 2. Experiments

PAN measurements were conducted at GCO (33.17°N, E126.10°E) on Jeju Island from October 10 to November 6, 2010. GCO is located on a cliff at the western edge of Jeju Island.

PAN was determined through fast gas chromatography (GC) with luminol chemiluminescence detection, which is described in detail elsewhere (Gaffney et al., 1998;

Atmos. Chem. Phys. Discuss., doi:10.5194/acp-2016-1107, 2017
Manuscript under review for journal Atmos. Chem. Phys.
Published: 25 January 2017


Atmospheric Chemistry and Physics Discussions

Lee et al., 2008; Marley et al., 2004). Here, we briefly describe the measurement method. Ambient air PAN and $NO_2$ (and peroxypropyl nitrate (PPN) if present) were separated along a 10-m capillary GC column (DB-1, J&W Scientific, Folsom, CA, USA), whose end was connected to a luminol cell where the column effluent reacted with luminol, giving off luminescent light (Lee et al., 2008; Lee et al., 2012). The concentrations of PAN and other species were determined from the chemiluminescence signals detected by a gated photon counter (HC135-01, Hamamatsu, Bridgewater, NJ, USA) at 425 nm, which was set at 800 V and operated at room temperature (Gaffney et al., 1998; Lee et al., 2012; Lee et al., 2008). PAN was calibrated against standards synthesized by the nitration of peracetic acid in n-tridecane (Gaffney et al., 1984; Gregory, 1990). The nominal detection limit of PAN defined by 3σ of the lowest standard was 100 pptv (Lee et al., 2008).

Water-soluble ions of $PM_{1.0}$ were collected by a particle-into-liquid sampler and analyzed by ion chromatography. Gaseous species, including $O_3$, NO, $NO_2$, CO, and $SO_2$, were measured by UV absorption, chemiluminescence with a molybdenum converter, non-dispersive infrared, and pulse UV fluorescence method, respectively (NIER, 2016). Aerosol species, including $PM_{10}$ mass and $PM_{2.5}$ OC and EC were measured and recorded along with meteorological parameters (relative humidity, temperature, and wind speed). The detailed results of the aerosol measurements can be found in Shang et al. (2017).

The three-day backward trajectories of air parcel at 850m a.s.l. for every one hour were calculated using NOAA Air Resources Laboratory (ARL) Hybrid Single-Particle Lagrangian Integrated Trajectory (HYSPLIT) model (version 4) (Draxler and Rolph, 2012; Rolph, 2012, http://www.arl.noaa.gov/ready/hysplit4.html).

## 3. Results

Atmos. Chem. Phys. Discuss., doi:10.5194/acp-2016-1107, 2017
Manuscript under review for journal Atmos. Chem. Phys.
Published: 25 January 2017


Atmospheric Chemistry and Physics Discussions

In the present experiments, PAN mixing ratios range from 0.1 to 2.4 ppbv, with an average of 0.6 ppbv. This mean value is lower than those observed in other Asian megacities: Beijing (1.41 ppb in the summer), Pearl River Delta region (1.32 ppb in the summer), and Seoul (0.8 ppb in the early summer); similar to those of suburban areas in China, e.g., Lanzhou (0.76 ppb in the summer); and higher than those in the western coast of the US, e.g., Sacramento (0.45 ppb in the summer), Mt. Bachelor (0.144 ppb in the spring and early summer), off the western coast of the US (0.65 ppb in the spring), and over the remote North Pacific (total PAN < 0.3 ppb in spring) (Bertram et al., 2013; Fischer et al., 2011; La Franchi et al., 2009; Lee et al., 2008; Roberts et al., 2004; Wang et al., 2010; Zhang et al., 2009; Zhang et al., 2011). Because the PAN lifetime is greatly dependent on temperature, its concentration decreases with increasing distance from the source regions. The PAN mixing ratios calculated in this study thus lie in-between the levels for the East Asian megacities and the northern Pacific. The distributions of all measured species, including PAN and $O_3$, are presented in Fig. 1. In particular, there are several periods characterized by high concentrations of PAN, $O_3$, and $PM_{10}$. In terms of PAN, four periods are particularly interesting (Fig. 1). High $O_3$ concentrations were observed during October 31–November 2 [episode 1] but did not coincide with high PAN concentrations. During October 28–29 [episode 2], $NO_2$ was noticeably increased. On the other hand, PAN and $O_3$ concentrations were both high during October 20–21 [episode 3] and November 4–5 [episode 4]. Episodes 3 and 4 are characterized by haze, while episodes 1 and 2 are characterized by urban influence in the Korean and Beijing outflows, respectively.

In the present study, PAN correlates reasonably well with $O_3$ ($\gamma$ = 0.67) and even better with $PM_{10}$ ($\gamma$ = 0.75). In general, $O_3$ and PAN exhibit typical diurnal variation with a maximum recorded in the afternoon, which results in a good correlation between the two

Atmos. Chem. Phys. Discuss., doi:10.5194/acp-2016-1107, 2017
Manuscript under review for journal Atmos. Chem. Phys.
Published: 25 January 2017


Atmospheric Chemistry and Physics Discussions

(Brasseur et al., 1999; Gaffney et al., 1999; Ridley et al., 1990; Schrimpf et al., 1995; Wang et al., 2010). In this study, however, the $O_3$ peak was often found in the early morning and late afternoon for several days (Fig. 1). Observing the diurnal variations in the entire PAN concentration measurement set (Fig. 2), the maximum was clearly recorded in the morning with the highest outliers, which is rather similar to that of $PM_{10}$. The diurnal pattern of $NO_2$ shows little variation, even though its concentrations were increased in the morning along with PAN. This first measurement of PAN at GCO reveals that PAN is not always coupled with $O_3$, which was not typically observed at remote sites in previous studies (e.g., Fischer et al., 2010; Lee et al., 2012).

## 4. Discussion

### 4.1. Decoupling of PAN from $O_3$

To examine the detailed mechanism of the decoupling of PAN from $O_3$, the daily maximum concentrations of PAN and $O_3$ were further explored. The recorded daily PAN maxima were generally in good correlation with $O_3$, albeit the relationship did not seem to hold at high concentrations of PAN and $O_3$ (Fig. 3). The daily maxima were then categorized into four groups according to the time when each $O_3$ and PAN maximum was recorded: "$O_3$ day-PAN day," "$O_3$ day-PAN night," "$O_3$ night-PAN day," and "$O_3$ night-PAN night." The day interval started from 08:00 and ended at 18:00 (local time), based on the times of sunrise and sunset during the experiment period. While the high PAN concentrations were associated with the "$O_3$ day-PAN day" group (cross symbols in Fig. 3), the enhanced $O_3$ concentration was recorded in the "$O_3$ night-PAN night" group (star symbols in Fig. 3). The "$O_3$ night-PAN night" group unexpectedly held more data points than the "$O_3$ day-PAN day" group, even though the "$O_3$ night-PAN night" group concentrations were lower (Fig. 3). In addition, there

Atmos. Chem. Phys. Discuss., doi:10.5194/acp-2016-1107, 2017
Manuscript under review for journal Atmos. Chem. Phys.
Published: 25 January 2017


Atmospheric Chemistry and Physics Discussions

were several days classified in the "$O_3$ night-PAN day" (marked by diamond) and "$O_3$ day-PAN night" groups, but with less frequency and lower concentrations. These results indicate that the decoupling of PAN from $O_3$ was primarily due to the elevated concentrations of $O_3$ and/or PAN at night. The four high PAN and $O_3$ episodes identified in this study fall under the category of "$O_3$ night-PAN night" or "$O_3$ day-PAN day." This point will be further examined to identify the chemical and physical processes responsible for PAN being decoupled from $O_3$, instead of being coupled with $PM_{10}$. The overall characteristics of the four episodes are summarized in Table 1.

### 4.2. Export of $O_3$ from Asian continents (episodes 1 & 2)

High $O_3$ concentrations were encountered around midnight on three consecutive days from October 31 to November 2 (episode 1), during which $SO_2$ reached its maximum concentration (Fig. 1). The backward trajectories of air masses revealed that air passed through the Beijing area during this period (Fig. 4). The wind was strong (13.5 m/s on average) and the recorded $O_3$ maximum (80.6 ppbv) was concurrent with the PAN maximum (0.9 ppbv) around midnight on November 1st (Fig. 4).

All these results indicate that the air was heavily influenced by outflow from the Beijing area, as previously hypothesized (Lim et al., 2012), and that the nighttime enhancement of $O_3$ and PAN resulted from the fast transport of relatively less-aged urban plumes. In this episode, PAN and $O_3$ could have been formed in urban areas or produced in the outflow while being transported. Because the overall correlation between $O_3$ and PAN was the best with the highest daily $\Delta O_3/\Delta PAN$ among all cases discussed in this study, episode 1 likely represents an event of rapid transport from the Beijing area (Fig. 5).

In previous studies, the nighttime enhancement of $O_3$ was observed at GCO (e.g., Lee et al., 2007) in association with pollutant-laden air coming from Beijing. Similarly, Banta et al.

Atmos. Chem. Phys. Discuss., doi:10.5194/acp-2016-1107, 2017
Manuscript under review for journal Atmos. Chem. Phys.
Published: 25 January 2017




(1998) pointed out that the evening $O_3$ maximum was due to long-range transport of $O_3$ from nearby urban areas. Wang et al. (2011) reported that the $O_3$ lifetime was about two days in East China during the summer, which is sufficient time for air to travel to GCO. Therefore, the nighttime maximum of $O_3$ can be attributed to the export of $O_3$ from megacities in China, causing PAN to be decoupled from $O_3$. Another night maximum of $O_3$ was recorded on October 29. Note that $NO_x$ was highly elevated during October 28–29 (episode 2) (Fig. 5b). In contrast, $O_3$ and PAN levels remained relatively low, leading to the lowest daily $\Delta O_3/\Delta PAN$ among all episodes. In this case, air masses passed through the Korean Peninsula, carrying low $O_3$ being titrated by high $NO_x$ (Brasseur et al., 1999; Jacobson, 2005).

### 4.3. PAN enhancement upon occurrence of haze (episodes 3 & 4)

In this study, two haze events were observed in the very beginning (October 20–21; episode 3) and the end of the study period (November 4–5; episode 4). The first haze event occurred on October 18th and lingered until October 21st, during which $O_3$ concentrations were gradually elevated. A second peak was recorded around midnight of October 19th and 20th, and the maximum was reached in the afternoon of October 20th (Figs. 1 and 3). In this episode, the maximum concentrations of $O_3$ and PAN were 78.9 ppbv and 2.0 ppbv, respectively, on October 29th, when the highest $NO_2$ concentration (12.7 ppbv) was observed under low wind speed (6.6 m/s daily average). The air mass trajectories suggest the influence of the Korean Peninsula, particularly the Seoul metropolitan area, in addition to East China (Fig. 4b).

In the second haze event (episode 4), an air mass was slowly transported from East China, including the Jiangsu province, under stagnant condition which was developed by an anticyclone system (Fig. 4). We measured the highest concentrations of all aerosol species

Atmos. Chem. Phys. Discuss., doi:10.5194/acp-2016-1107, 2017
Manuscript under review for journal Atmos. Chem. Phys.
Published: 25 January 2017


Atmospheric Chemistry and Physics Discussions

including the $PM_{10}$ mass as well as PAN and $O_3$, which were 170 μg/m$^3$, 2.4 ppbv, and 87.5 ppbv, respectively. Other reactive gases such as CO, $SO_2$, and $NO_2$ were also highly elevated. Note that PAN and $O_3$ gradually increased through the night, leading to a nighttime maximum of both species on November 4th. It is likely that the pre-formed PAN and $O_3$ were continuously transported into Gosan at night.

In section 4.2, the nighttime $O_3$ peak was attributed to the transport from nearby urban areas to Jeju Island. The two haze episodes were also observed in continental outflows. Unlike $O_3$, however, PAN is linearly correlated with the $PM_{10}$ mass and major constituents of aerosols including $PM_{2.5}$ OC, $PM_{2.5}$ EC, and $PM_{1.0}$ $K^+$, whose concentrations were remarkably high in this episode.

PAN is formed through the reaction of the peroxyacetyl radical and nitrogen dioxide (Eq. 1) and decomposed at high temperature (Eq. 2), returning these radicals. Unless the NO concentration is high (Eq. 3), the peroxyacetyl radical recombines with $NO_2$, producing PAN. Thus, the total lifetime of PAN depends on the $NO_2$/NO ratio and temperature (Eq. 4) (Brasseur et al., 1999).

$$CH_3C(O)O_2 + NO_2 + M \rightarrow PAN + M \quad (1)$$

$$PAN \rightarrow CH_3C(O)O_2 + NO_2 \quad (2)$$

$$CH_3C(O)O_2 + NO \rightarrow CH_3CO_2 + NO_2 \quad (3)$$

$$T_{eff} = T_d \left(1 + \frac{k_1[NO_2]}{k_2[NO]}\right) \ [sec^{-1}] \quad (4)$$

where $T_d$ and $T_{eff}$ indicate the lifetime against decomposition and the effective lifetime of PAN (Brasseur et al., 1999). The effective lifetime of PAN was estimated through Eq. 4 using the rate constants proposed by Brasseur et al. (1999), Jacobson (2005), and Maricq and Szente (1996).

During the haze event, NO was close to the detection limit, while $NO_2$ was greatly enhanced. Owing to the high $NO_2$/NO ratio, the effective lifetime of PAN increased by 57

Atmos. Chem. Phys. Discuss., doi:10.5194/acp-2016-1107, 2017
Manuscript under review for journal Atmos. Chem. Phys.
Published: 25 January 2017




239 times; this possibly contributed to the gradual increase in PAN through the night on
240 November 4th. In an aged plume, $NO_2$ is likely to be recycled with $O_3$ during the day and
241 PAN during the night. Fischer et al. (2014) also reported that, at night, PAN can be produced
242 from the reaction of acetaldehyde with the nitrate radical.

243 Besides $PM_{10}$, PAN was also well correlated with $PM_{2.5}$ OC and EC not only during this
244 haze episode but also during the entire measurement period (Fig. 6b and c). Furthermore, the
245 enhancement of PAN was concurrent with that of OC and $K^+$, resulting in excellent
246 correlation between them (Fig. 6e and f). In fact, the $\Delta OC/\Delta EC$ ratio of episode 4 was much
247 higher (7) than those of the other episodes (~2.5) (Fig. 6d). The fraction of $PM_{2.5}$ against
248 $PM_{10}$ was also the highest in this episode, indicating significant contribution of secondary
249 aerosols. These observations suggest that air masses were affected by biomass combustion
250 (e.g., Ram et al., 2008, 2012; Saarikoski et al., 2008).

251 According to previous studies, PAN can be produced in plumes through biomass
252 combustion (Alvarado et al., 2010; Coheur et al., 2007; Liu et al., 2016; Tereszchuk et al.,
253 2013). In northeast China, open burnings related to agricultural activities frequently occur
254 during the spring and fall (Duan et al., 2004; Yang et al., 2005). Kudo et al. (2014) also
255 reported that, upon burning crop residue in Yangtze region, the levels of oxygenated VOCs
256 were elevated together with $NO_x$. In addition, biofuel is used for cooking and heating and as
257 an energy source in China's industry (Cao et al., 2006).

258 Therefore, PAN is likely to increase when haze occurs and fine aerosols are transformed as
259 air masses carrying combustion emissions are slowly transported from China over the Yellow
260 Sea. Additionally, the results of this study imply that PAN can be used as a robust tracer for
261 continental outflows in northeast Asia, to identify transport- and chemical transformation-
262 dominant regimes. In a transport-dominant regime, $O_3$ export was distinguished by the

Atmos. Chem. Phys. Discuss., doi:10.5194/acp-2016-1107, 2017
Manuscript under review for journal Atmos. Chem. Phys.
Published: 25 January 2017


Atmospheric Chemistry and Physics Discussions

highest levels of primary gaseous species such as $SO_2$ and relatively low levels of PAN. In contrast, fine aerosol species are enhanced in a chemical transformation regime, leading to haze events with relatively more enhanced PAN compared to $O_3$.

Finally, the measured $O_3$ and PAN concentrations were compared to results from a global chemistry model, the Community Atmosphere Model with Chemistry (CAM-Chem), a component of the Community Earth System Model (CESM) (Lamarque et al., 2012; Tilmes et al., 2015). The CAM-chem results shown here follow the configuration used for the HTAP2 (Hemispheric Transport of Air Pollution, Phase 2) intercomparison (e.g., Stjern et al., 2016). CAM-chem is nudged to observed meteorology (GEOS-5) to reproduce the actual period of the observations (Oct 2010). The emissions used in the model are the HTAP2 inventory (Janssens-Maenhout, et al., 2015), which include the "MIX" Asian emissions inventory. Biomass burning emissions are from the Global Fire Emissions Database (GFED3) (Randerson et al., 2013). In the model simulation, $O_3$ and PAN were highly underestimated during the episodes observed in Chinese outflows, although the variation around average level of $O_3$ and PAN was well captured (Fig. 7). The enhancement of PAN during the haze events was not well represented in the model (Oct 20–21 and Nov 4–5). The timing of the $O_3$ diurnal variability was captured by the model, although the magnitude of the variation was underestimated. These results reveal that the current understanding of Chinese outflow is still not sufficient, thereby causing uncertainty in estimating its effect on air quality in the northwestern Pacific Rim.

Atmos. Chem. Phys. Discuss., doi:10.5194/acp-2016-1107, 2017
Manuscript under review for journal Atmos. Chem. Phys.
Published: 25 January 2017


Atmospheric Chemistry and Physics Discussions

## 5. Conclusions

The first measurements of PAN, reactive gases, and aerosol species were conducted at GCO during October 19 to November 6, 2010. The average concentration of PAN was 0.6 ppbv with a maximum of 2.4 ppbv, which was lower than those in major cities in East Asia but much higher than the background concentrations in other regions. In addition, PAN and $O_3$ concentrations were well correlated ($\gamma$ = 0.67). However, the comparison of the daily maxima of PAN and $O_3$ highlighted that they were not proportionally enhanced. That is, either PAN was relatively more elevated than $O_3$ or the highest $O_3$ was associated with low levels of PAN. Unexpectedly, both PAN and $O_3$ often reached their maxima at night. As a result, PAN was decoupled from $O_3$ and better correlated with the $PM_{10}$ mass ($\gamma$ = 0.75) than with $O_3$. In this study, these high-concentration episodes were all encountered in association with continental outflows, and thus, two high-$O_3$ and two high-PAN events were recorded and investigated in detail.

During the $O_3$ episodes, both $O_3$ and PAN concentrations reached their maximum values at night. In episode 1 (Oct. 31 to Nov. 2), the $O_3$ concentration was increased to 80.6 ppbv, with a high $SO_2$ concentration under strong wind. It was a typical Beijing plume observed in the study region. In comparison, $NO_2$ was greatly increased in episode 2 (Oct. 28–29) when the air masses were affected by urban emissions from Korean Peninsula. Although the maximum $O_3$ level was lower during episode 2, these two cases demonstrated well how $O_3$ was exported from the East Asian continent.

The remaining two episodes were highlighted by enhanced PAN concentrations and characterized by haze occurrence. During episode 3 (Oct. 20–21), PAN and $O_3$ concentrations increased up to 2.0 ppbv and 78.9 ppbv, respectively, with high NOx levels, probably influenced by emissions from Korea. Episode 4 (Nov. 4–5) was characterized by the highest

Atmos. Chem. Phys. Discuss., doi:10.5194/acp-2016-1107, 2017
Manuscript under review for journal Atmos. Chem. Phys.
Published: 25 January 2017




concentrations of almost all measured species, including PAN, $O_3$, $PM_{10}$ mass, and $PM_{1.0}$ species; the maximum recorded concentrations of PAN, $O_3$, and $PM_{10}$ mass during this interval were 2.4 ppbv, 87.5 ppbv, and 170 $\mu g/m^3$, respectively. Note that, along with $PM_{10}$ and $O_3$, PAN was gradually increased through the night. In this episode, an air mass was slowly transported from eastern China. With depleted NO, the effective lifetime of PAN was greatly extended. In addition, PAN concentration showed good correlation with OC, EC, and $K^+$; in fact, the correlation of PAN with $K^+$ was comparable to that of OC with $K^+$. These results, in conjunction with the high $\Delta OC/\Delta EC$ (7), imply that the observed haze was mainly caused by the emissions produced by biomass combustion. These results suggest that PAN is a useful tool for distinguishing continental outflows that were typically observed in northeast Asia.

The comparison between the measured and calculated concentrations using the CAM-Chem-HTAP2 model showed that the model underestimated the $O_3$ and PAN levels in Chinese outflows, particularly for haze incidence. These results reveal that Chinese outflows are still poorly understood and not well captured in the model.

**Acknowledgments**

This study was funded by the Korea Meteorological Administration Research and Development Program under Grant KMIPA 2015-6020. The National Center for Atmospheric Research is funded by the National Science Foundation. The authors gratefully acknowledge the NOAA Air Resources Laboratory (ARL) for the provision of the HYSPLIT transport and dispersion model and/or READY website (http://www.ready.noaa.gov) used in this publication.

Atmos. Chem. Phys. Discuss., doi:10.5194/acp-2016-1107, 2017
Manuscript under review for journal Atmos. Chem. Phys.
Published: 25 January 2017


Atmospheric Chemistry and Physics Discussions

330 **References**

331 Akimoto, H.: Global air quality and pollution, Science, 302, 1716-1719,
332 doi:10.1126/science.1092666, 2003.

333 Alvarado, M. J., Logan, J. A., Mao, J., Apel, E., Riemer, D., Blake, D., Cohen, R. C., Min, K.
334 E., Perring, A. E., Browne, E. C., Wooldridge, P. J., Diskin, G. S., Sachse, G. W.,
335 Fuelberg, H., Sessions, W. R., Harrigan, D. L., Huey, G., Liao, J., Case-Hanks, A.,
336 Jimenez, J. L., Cubison, M. J., Vay, S. A., Weinheimer, A. J., Knapp, D. J., Montzka, D.
337 D., Flocke, F. M., Pollack, I. B., Wennberg, P. O., Kurten, A., Crounse, J., Clair, J. M. S.,
338 Wisthaler, A., Mikoviny, T., Yantosca, R. M., Carouge, C. C., and Le Sager, P.: Nitrogen
339 oxides and PAN in plumes from boreal fires during ARCTAS-B and their impact on
340 ozone: an integrated analysis of aircraft and satellite observations, Atmos. Chem. Phys.,
341 10, 9739-9760, doi:10.5194/acp-10-9739-2010, 2010.

342 Aneja, V. P., Hartsell, B. E., Kim, D. S., and Grosjean, D.: Peroxyacetyl nitrate in Atlanta,
343 Georgia: Comparison and analysis of ambient data for suburban and downtown
344 locations, J. Air & Waste Manage. Assoc., 49, doi: 177-184,
345 10.1080/10473289.1999.10463786, 1999.

346 Banta, R. M., Senff, C. J., White, A. B., Trainer, M., McNider, R. T., Valente, R. J., Mayor, S.
347 D., Alvarez, R. J., Hardesty, R. M., Parrish, D., and Fehsenfeld, F. C.: Daytime buildup
348 and nighttime transport of urban ozone in the boundary layer during a stagnation episode,
349 J. Geophys. Res. Atmos., 103, 22519-22544, doi:10.1029/98jd01020, 1998.

350 Beine, H. J., Jaffe, D. A., Herring, J. A., Kelley, J. A., Krognes, T., and Stordal, F.: High-
351 latitude springtime photochemistry .1. NOx, PAN and ozone relationships, J. Atmos.
352 Chem., 27, 127-153, doi:10.1023/a:1005869900567, 1997.

353 Bertram, T. H., Perring, A. E., Wooldridge, P. J., Dibb, J., Avery, M. A., and Cohen, R. C.: On
354 the export of reactive nitrogen from Asia: $NO_x$ partitioning and effects on ozone, Atmos.
355 Chem. Phys., 13, 4617-4630, doi:10.5194/acp-13-4617-2013, 2013.

356 Brasseur, G. P., Orlando, J. J., and Tyndall, G. S.: Atmospheric chemistry and global change,
357 Oxford University Press, New York, 235-347 pp., 1999.

358 Cao, G., Zhang, X., and Zheng, F.: Inventory of black carbon and organic carbon emissions
359 from China, Atmos. Environ., 40, 6516-6527, doi:10.1016/j.atmosenv.2006.05.070,
360 2006.

361 Coheur, P. F., Herbin, H., Clerbaux, C., Hurtmans, D., Wespes, C., Carleer, M., Turquety, S.,
362 Rinsland, C. P., Remedios, J., Hauglustaine, D., Boone, C. D., and Bernath, P. F.: ACE-
363 FTS observation of a young biomass burning plume: first reported measurements of
364 $C_2H_4$, $C_3H_6O$, $H_2CO$ and PAN by infrared occultation from space, Atmos. Chem. Phys.,
365 7, 5437-5446, doi:10.5194/acp-7-5437-2007, 2007.

366 Draxler, R. R., and Rolph, G. D.: HYSPLIT (HYbrid Single-Particle Lagrangian Integrated
367 Trajectory) Model access via NOAA ARL READY Website
368 (http://ready.arl.noaa.gov/HYSPLIT.php), NOAA Air Resources Laboratory, Silver
369 Spring, MD., 2012.

370 Duan, F., Liu, X., Yu, T., and Cachier, H.: Identification and estimate of biomass burning
371 contribution to the urban aerosol organic carbon concentrations in Beijing, Atmos.
372 Environ., 38, 1275-1282, doi:10.1016/j.atmosenv.2003.11.037, 2004.



373 Fischer, E. V., Jaffe, D. A., Reidmiller, D. R., and Jaeglé, L.: Meteorological controls on
374 observed peroxyacetyl nitrate at Mount Bachelor during the spring of 2008, J. Geophys.
375 Res., 115, D03302, doi:10.1029/2009jd012776, 2010.

376 Fischer, E. V., Jaffe, D. A., and Weatherhead, E. C.: Free tropospheric peroxyacetyl nitrate
377 (PAN) and ozone at Mount Bachelor: potential causes of variability and timescale for
378 trend detection, Atmos. Chem. Phys., 11, 5641-5654, doi:10.5194/acp-11-5641-2011,
379 2011.

380 Fischer, E. V., Jacob, D. J., Yantosca, R. M., Sulprizio, M. P., Millet, D. B., Mao, J., Paulot, F.,
381 Singh, H. B., Roiger, A., Ries, L., Talbot, R. W., Dzepina, K., and Pandey, D. S.:
382 Atmospheric peroxyacetyl nitrate (PAN): a global budget and source attribution, Atmos.
383 Chem. Phys., 14, 2679-2698, doi:10.5194/acp-14-2679-2014, 2014.

384 Gaffney, J. S., Fajer, R., and Senum, G. I.: An improved procedure for high purity gaseous
385 peroxyacyl nitrate production: Use of heavy lipid solvents, Atmos. Environ., 18, 215-
386 218, doi:10.1016/0004-6981(84)90245-2, 1984.

387 Gaffney, J. S., Bornick, R. M., Chen, Y. H., and Marley, N. A.: Capillary gas chromatographic
388 analysis of nitrogen dioxide and pans with luminol chemiluminescent detection, Atmos.
389 Environ., 32, 1445-1454, doi:10.1016/S1352-2310(97)00098-8, 1998.

390 Gaffney, J. S., Marley, N. A., Cunningham, M. M., and Doskey, P. V.: Measurements of
391 peroxyacyl nitrates (PANs) in Mexico City: implications for megacity air quality
392 impacts on regional scales, Atmos. Environ., 33, 5003-5012, doi:10.1016/S1352-
393 2310(99)00263-0, 1999.

394 Gallagher, M. S., Carsey, T. P., and Farmer, M. L.: Peroxyacetyl nitrate in the North Atlantic
395 marine boundary layer, Global Biogeochem. Cycle., 4, 297-308,
396 doi:10.1029/GB004i003p00297, 1990.

397 Gregory, G. L.: An intercomparison of airborne PAN measurements, J. Geophys. Res., 95,
398 10077-10087, doi:10.1029/JD095iD07p10077, 1990.

399 Grosjean, E., Grosjean, D., Woodhouse, L. F., and Yang, Y.-J.: Peroxyacetyl nitrate and
400 peroxypropionyl nitrate in Porto Alegre, Brazil, Atmos. Environ., 36, 2405-2419,
401 doi:10.1016/S1352-2310(01)00541-6, 2002.

402 Hansel, A., and Wisthaler, A.: A method for real-time detection of PAN, PPN and MPAN in
403 ambient air, Geophys. Res. Lett., 27, 895-898, doi:10.1029/1999gl010989, 2000.

404 Jacob, D. J.: Introduction to atmospheric chemistry, 199-231 pp., 1999.

405 Jacob, D. J.: Heterogeneous chemistry and tropospheric ozone, Atmos. Environ., 34, 2131-
406 2159, doi:10.1016/s1352-2310(99)00462-8, 2000.

407 Jacobson, M. Z.: Fundamentals of atmospheric modeling, Second edition, Cambridge, UK,
408 731-738 pp., 2005.

409 Jaffe, D. A., Thornton, J., Wolfe, G., Reidmiller, D., Fischer, E. V., Jacob, D. J., Zhang, L.,
410 Cohen, R., Singh, H., Weinheimer, A., and Flocke, F.: Can we detect an Influence over
411 North America from Increasing Asian NOx Emissions?, Eos Trans, AGU, 88, 2007.

412 Janssens-Maenhout, G., Crippa, M., Guizzardi, D., Dentener, F., Muntean, M., Pouliot, G.,
413 Keating, T., Zhang, Q., Kurokawa, J., Wankmüller, R., Denier van der Gon, H., Kuenen,
414 J. J. P., Klimont, Z., Frost, G., Darras, S., Koffi, B., and Li, M.: HTAP_v2.2: a mosaic of



regional and global emission grid maps for 2008 and 2010 to study hemispheric transport of air pollution, Atmos. Chem. Phys., 15, 11411-11432, doi:10.5194/acp-15-11411-2015, 2015.

Kanaya, Y., Tanimoto, H., Matsumoto, J., Furutani, H., Hashimoto, S., Komazaki, Y., Tanaka, S., Yokouchi, Y., Kato, S., Kajii, Y., and Akimoto, H.: Diurnal variations in $H_2O_2$, $O_3$, PAN, $HNO_3$ and aldehyde concentrations and $NO/NO_2$ ratios at Rishiri Island, Japan: Potential influence from iodine chemistry, Sci. Total Envir., 376, 185-197, doi:10.1016/j.scitotenv.2007.01.073, 2007.

Kenley, R. A., and Hendry, D. G.: Generation of peroxy radicals from peroxynitrates ($ROONO_2$). Decomposition of peroxybenzoyl nitrate (PBzN), J. Am. Chem. Soc., 104, 220-224, doi:10.1021/ja00365a040, 1982.

Kudo, S., Tanimoto, H., Inomata, S., Saito, S., Pan, X., Kanaya, Y., Taketani, F., Wang, Z., Chen, H., Dong, H., Zhang, M., and Yamaji, K.: Emissions of nonmethane volatile organic compounds from open crop residue burning in the Yangtze River Delta region, China, J. Geophys. Res., 119, 7684–7698, doi:10.1002/2013JD021044, 2014.

LaFranchi, B. W., Wolfe, G. M., Thornton, J. A., Harrold, S. A., Browne, E. C., Min, K. E., Wooldridge, P. J., Gilman, J. B., Kuster, W. C., Goldan, P. D., De Gouw, J. A., McKay, M., Goldstein, A. H., Ren, X., Mao, J., and Cohen, R. C.: Closing the peroxy acetyl nitrate budget: Observations of acyl peroxy nitrates (PAN, PPN, and MPAN) during BEARPEX 2007, Atmos. Chem. Phys., 9, 7623-7641, doi:10.5194/acp-9-7623-2009, 2009.

Lamarque, J. F., Emmons, L. K., Hess, P. G., Kinnison, D. E., Tilmes, S., Vitt, F., Heald, C. L., Holland, E. A., Lauritzen, P. H., Neu, J., Orlando, J. J., Rasch, P. J., and Tyndall, G. K.: CAM-chem: description and evaluation of interactive atmospheric chemistry in the Community Earth System Model, Geosci. Model Dev., 5, 369-411, doi:10.5194/gmd-5-369-2012, 2012.

Lee, G., Jang, Y., Lee, H., Han, J.-S., Kim, K.-R., and Lee, M.: Characteristic behavior of peroxyacetyl nitrate (PAN) in Seoul megacity, Korea, Chemosphere, 73, 619-628, doi:10.1016/j.chemosphere.2008.05.060, 2008.

Lee, G., Choi, H.-S., Lee, T., Choi, J., Park, J. S., and Ahn, J. Y.: Variations of regional background peroxyacetyl nitrate in marine boundary layer over Baengyeong Island, South Korea, Atmos. Environ., 61, 533-541, doi:10.1016/j.atmosenv.2012.07.075, 2012.

Lee, M., Song, M., Moon, K. J., Han, J. S., Lee, G., and Kim, K.-R.: Origins and chemical characteristics of fine aerosols during the northeastern Asia regional experiment (Atmospheric Brown Cloud-East Asia Regional Experiment 2005), J. Geophys. Res., 112, D22S29, doi:10.1029/2006jd008210, 2007.

Li, M., Zhang, Q., Kurokawa, J., Woo, J. H., He, K. B., Lu, Z., Ohara, T., Song, Y., Streets, D. G., Carmichael, G. R., Cheng, Y. F., Hong, C. P., Huo, H., Jiang, X. J., Kang, S. C., Liu, F., Su, H., and Zheng, B.: MIX: a mosaic Asian anthropogenic emission inventory for the MICS-Asia and the HTAP projects, Atmos. Chem. Phys. Discuss., 2015, 34813-34869, doi:10.5194/acpd-15-34813-2015, 2015.

Lim, S., Lee, M., Lee, G., Kim, S., Yoon, S., and Kang, K.: Ionic and carbonaceous compositions of $PM_{10}$, $PM_{2.5}$ and $PM_{1.0}$ at Gosan ABC Superstation and their ratios as source signature, Atmos. Chem. Phys., 12, 2007-2024, doi:10.5194/acp-12-2007-2012,



459 2012.

460 Liu, Z., Wang, Y., Gu, D., Zhao, C., Huey, L. G., Stickel, R., Liao, J., Shao, M., Zhu, T., Zeng,
461 L., Liu, S.-C., Chang, C.-C., Amoroso, A., and Costabile, F.: Evidence of reactive
462 aromatics as a major source of peroxy acetyl nitrate over China, Environ. Sci. Technol.,
463 44, 7017-7022, doi:10.1021/es1007966, 2010.

464 Liu, X., Zhang, Y., Huey, L. G., Yokelson, R. J., Wang, Y., Jimenez, J. L., Campuzano-Jost, P.,
465 Beyersdorf, A. J., Blake, D. R., Choi, Y., St. Clair, J. M., Crounse, J. D., Day, D. A.,
466 Diskin, G. S., Fried, A., Hall, S. R., Hanisco, T. F., King, L. E., Meinardi, S., Mikoviny,
467 T., Palm, B. B., Peischl, J., Perring, A. E., Pollack, I. B., Ryerson, T. B., Sachse, G.,
468 Schwarz, J. P., Simpson, I. J., Tanner, D. J., Thornhill, K. L., Ullmann, K., Weber, R. J.,
469 Wennberg, P. O., Wisthaler, A., Wolfe, G. M., and Ziemba, L. D.: Agricultural fires in
470 the southeastern U.S. during SEAC4RS: Emissions of trace gases and particles and
471 evolution of ozone, reactive nitrogen, and organic aerosol, Journal of Geophysical
472 Research: Atmospheres, 121, 7383-7414, doi:10.1002/2016JD025040, 2016.

473 Maricq, M. M., and Szente, J. J.: Temperature-dependent study of the $CH_3C(O)O_2$ + NO
474 reaction, J. Phys. Chem., 100, 12380-12385, doi:10.1021/jp960792c, 1996.

475 Marley, N. A., Gaffney, J. S., White, R. V., Rodriguez-Cuadra, L., Herndon, S. E., Dunlea, E.,
476 Volkamer, R. M., Molina, L. T., and Molina, M. J.: Fast gas chromatography with
477 luminol chemiluminescence detection for the simultaneous determination of nitrogen
478 dioxide and peroxyacetyl nitrate in the atmosphere, Rev. Sci. Instr., 75, 4595-4605,
479 doi:10.1063/1.1805271, 2004.

480 Mills, G. P., Sturges, W. T., Salmon, R. A., Bauguitte, S. J. B., Read, K. A., and Bandy, B. J.:
481 Seasonal variation of peroxyacetylnitrate (PAN) in coastal Antarctica measured with a
482 new instrument for the detection of sub-part per trillion mixing ratios of PAN, Atmos.
483 Chem. Phys., 7, 4589-4599, doi:10.5194/acp-7-4589-2007, 2007.

484 Muller, K. P., and Rudolph, J.: Measurements of peroxyacetylnitrate in the marine boundary
485 layer over the Atlantic, J. Atmos. Chem., 15, 361-367, doi:10.1007/BF00115405, 1992.

486 Nielsen, T., Samuelsson, U., Grennfelt, P., and Thomsen, E. L.: Peroxyacetyl nitrate in long-
487 range transported polluted air, Nature, 293, 553-555, doi:10.1038/293553a0, 1981.

488 NIER, 2016, Annual Report of Ambient Air Quality in Korea, 2015, National Institute of
489 Environmental Research, Inchon, Korea, p.10 (in Korean).

490 Ohara, T., Akimoto, H., Kurokawa, J., Horii, N., Yamaji, K., Yan, X., and Hayasaka, T.: An
491 Asian emission inventory of anthropogenic emission sources for the period 1980-2020,
492 Atmos. Chem. Phys., 7, 4419-4444, doi:10.5194/acp-7-4419-2007, 2007.

493 Ram, K., Sarin, M. M., and Hegde, P.: Atmospheric abundances of primary and secondary
494 carbonaceous species at two high-altitude sites in India: Sources and temporal variability,
495 Atmos. Environ., 42, 6785-6796, doi:10.1016/j.atmosenv.2008.05.031, 2008.

496 Ram, K., Sarin, M. M., and Tripathi, S. N.: Temporal trends in atmospheric $PM_{2.5}$, $PM_{10}$,
497 elemental carbon, organic carbon, water-soluble organic carbon, and optical properties:
498 Impact of biomass burning emissions in the Indo-Gangetic Plain, Environ. Sci. Technol.,
499 46, 686-695, doi:10.1021/es202857w, 2012.

500 Randerson, J. T., van der Werf, G. R., Giglio, L., Collatz, G. J., and Kasibhatla, P. S.: Global
501 Fire Emissions Database, Version 3 (GFEDv3.1). Data set. Available on-line



[http://daac.ornl.gov/] from Oak Ridge National Laboratory Distributed Active Archive Center, Oak Ridge, Tennessee, USA. doi:10.3334/ORNLDAAC/1191, 2013.

Ridley, B. A., Shetter, J. D., Gandrud, B. W., Salas, L. J., Singh, H. B., Carroll, M. A., Hubler, G., Albritton, D. L., Hastie, D. R., Schiff, H. I., Mackay, G. I., Karechi, D. R., Davis, D. D., Bradshaw, J. D., Rodgers, M. O., Sandholm, S. T., Torres, A. L., Condon, E. P., Gregory, G. L., and Beck, S. M.: Ratios of peroxyacetyl nitrate to active nitrogen observed during aircraft flights over the Eastern Pacific Oceans and continental United-States, J. Geophys. Res., 95, 10179-10192, doi:10.1029/JD095iD07p10179, 1990.

Roberts, J. M., Flocke, F., Chen, G., de Gouw, J., Holloway, J. S., Hübler, G., Neuman, J. A., Nicks, D. K., Nowak, J. B., Parrish, D. D., Ryerson, T. B., Sueper, D. T., Warneke, C., and Fehsenfeld, F. C.: Measurement of peroxycarboxylic nitric anhydrides (PANs) during the ITCT 2K2 aircraft intensive experiment, Journal of Geophysical Research: Atmospheres, 109, D23S21, doi:10.1029/2004JD004960, 2004.

Roberts, J. M., Marchewka, M., Bertman, S. B., Sommariva, R., Warneke, C., de Gouw, J., Kuster, W., Goldan, P., Williams, E., Lerner, B. M., Murphy, P., and Fehsenfeld, F. C.: Measurements of PANs during the New England Air Quality Study 2002, J. Geophys. Res., 112, D20306, doi:10.1029/2007JD008667, 2007.

Rolph, G. D.: Real-time Environmental Applications and Display sYstem (READY) Website (http://ready.arl.noaa.gov). NOAA Air Resources Laboratory, Silver Spring, MD. , 2012.

Saarikoski, S., Timonen, H., Saarnio, K., Aurela, M., Ĭrvi, L., Keronen, P., Kerminen, V. M., and Hillamo, R.: Sources of organic carbon in fine particulate matter in northern European urban air, Atmos. Chem. Phys., 8, 6281-6295, doi:10.5194/acp-8-6281-2008, 2008.

Schrimpf, W., Muller, K. P., Johnen, F. J., Lienaerts, K., and Rudolph, J.: An optimized method for airborne peroxyacetyl nitrate (PAN) measurements, J. Atmos. Chem., 22, 303-317, doi:10.1007/bf00696640, 1995.

Shang, X., Lee, M., Han, J., Kang, E., Gustafsson, Ö., Chang, I.-S., and Han, J.-S.: Water-soluble inorganic and organic compositions of submicron particles observed in Chinese outflows at Gosan Climate Observatory in spring and fall, soon to be submitted.

Staudt, A. C., Jacob, D. J., Ravetta, F., Logan, J. A., Bachiochi, D., Sandholm, S., Ridley, B., Singh, H. B., and Talbot, B.: Sources and chemistry of nitrogen oxides over the tropical Pacific, J. Geophys. Res., 108, 8239, doi:10.1029/2002JD002139, 2003.

Stjern, C. W., Samset, B. H., Myhre, G., Bian, H., Chin, M., Davila, Y., Dentener, F., Emmons, L., Flemming, J., Haslerud, A. S., Henze, D., Jonson, J. E., Kucsera, T., Lund, M. T., Schulz, M., Sudo, K., Takemura, T., and Tilmes, S.: Global and regional radiative forcing from 20% reductions in BC, OC and SO4 – an HTAP2 multi-model study, Atmos. Chem. Phys., 16, 13579-13599, doi:10.5194/acp-16-13579-2016, 2016.

Talukdar, R. K., Burkholder, J. B., Schmoltner, A. M., Roberts, J. M., Wilson, R. R., and Ravishankara, A. R.: Investigation of the loss processes for peroxyacetyl nitrate in the atmosphere: UV photolysis and reaction with OH, J. Geophys. Res., 100, 14163-14173, doi:10.1029/95JD00545, 1995.

Tereszchuk, K. A., Moore, D. P., Harrison, J. J., Boone, C. D., Park, M., Remedios, J. J., Randel, W. J., and Bernath, P. F.: Observations of peroxyacetyl nitrate (PAN) in the



upper troposphere by the Atmospheric Chemistry Experiment-Fourier Transform Spectrometer (ACE-FTS), Atmos. Chem. Phys., 13, 5601-5613, doi:10.5194/acp-13-5601-2013, 2013.

Tilmes, S., Lamarque, J. F., Emmons, L. K., Kinnison, D. E., Ma, P. L., Liu, X., Ghan, S., Bardeen, C., Arnold, S., Deeter, M., Vitt, F., Ryerson, T., Elkins, J. W., Moore, F., Spackman, J. R., and Val Martin, M.: Description and evaluation of tropospheric chemistry and aerosols in the Community Earth System Model (CESM1.2), Geosci. Model Dev., 8, 1395-1426, doi:10.5194/gmd-8-1395-2015, 2015.

Wang, B., Shao, M., Roberts, J. M., Yang, G., Yang, F., Hu, M., Zeng, L., Zhang, Y., and Zhang, J.: Ground-based on-line measurements of peroxyacetyl nitrate (PAN) and peroxypropionyl nitrate (PPN) in the Pearl River Delta, China, Int. J. Environ. Anal. Chem., 90, 548-559, doi:10.1080/03067310903194972, 2010.

Wang, Y., Zhang, Y., Hao, J., and Luo, M.: Seasonal and spatial variability of surface ozone over China: contributions from background and domestic pollution, Atmos. Chem. Phys., 11, 3511-3525, doi:10.5194/acp-11-3511-2011, 2011.

Yang, F., He, K., Ye, B., Chen, X., Cha, L., Cadle, S. H., Chan, T., and Mulawa, P. A.: One-year record of organic and elemental carbon in fine particles in downtown Beijing and Shanghai, Atmos. Chem. Phys., 5, 1449-1457, doi:10.5194/acp-5-1449-2005, 2005.

Zhang, H., Xu, X., Lin, W., and Wang, Y.: Wintertime peroxyacetyl nitrate (PAN) in the megacity Beijing: Role of photochemical and meteorological processes, J. Environ. Sci., 26, 83-96, doi:10.1016/S1001-0742(13)60384-8, 2014.

Zhang, J. B., Xu, Z., Yang, G., and Wang, B.: Peroxyacetyl nitrate (PAN) and peroxypropionyl nitrate (PPN) in urban and suburban atmospheres of Beijing, China, Atmos. Chem. Phys. Discuss., 11, 8173-8206, doi:10.5194/acpd-11-8173-2011, 2011.

Zhang, J. M., Wang, T., Ding, A. J., Zhou, X. H., Xue, L. K., Poon, C. N., Wu, W. S., Gao, J., Zuo, H. C., Chen, J. M., Zhang, X. C., and Fan, S. J.: Continuous measurement of peroxyacetyl nitrate (PAN) in suburban and remote areas of western China, Atmos. Environ., 43, 228-237, doi:10.1016/j.atmosenv.2008.09.070, 2009.

Zhang, L., Jacob, D. J., Boersma, K. F., Jaffe, D. A., Olson, J. R., Bowman, K. W., Worden, J. R., Thompson, A. M., Avery, M. A., Cohen, R. C., Dibb, J. E., Flock, F. M., Fuelberg, H. E., Huey, L. G., McMillan, W. W., Singh, H. B., and Weinheimer, A. J.: Transpacific transport of ozone pollution and the effect of recent Asian emission increases on air quality in North America: An integrated analysis using satellite, aircraft, ozonesonde, and surface observations, Atmos. Chem. Phys., 8, 6117-6136, doi:10.5194/acp-8-6117-2008, 2008.

Atmos. Chem. Phys. Discuss., doi:10.5194/acp-2016-1107, 2017
Manuscript under review for journal Atmos. Chem. Phys.
Published: 25 January 2017


Atmospheric Chemistry and Physics Discussions

580 **Tables**

581

582 Table 1. Chemical and meteorological characteristics of the four episodes.

| | Episode 1 | Episode 2 | Episode 3 | Episode 4 |
|---|---|---|---|---|
| Type | Transport dominant | Transport dominant | Chemical transformation | Chemical transformation |
| Event | $O_3$ export | $O_3$ export | Haze | Haze |
| $O_3$ (ppbv) | 60.2 (80.6) | 45.6 (62.8) | 59.7 (78.9) | 61.8 (87.5) |
| PAN (ppbv) | 0.5 (0.9) | 0.5 (0.8) | 1.2 (2.0) | 1.3 (2.4) |
| $PM_{10}$ ($\mu g/m^3$) | 57 (90) | 38 (56) | 69 (96) | 100 (170) |
| $SO_2$ (ppbv) | 4.3 (12.9) | 2.0 (4.4) | 2.6 (5.4) | 4.4 (9.5) |
| $NO_2$ (ppbv) | 3.7 (7.3) | 6.2 (12.1) | 6.2 (12.7) | 6.1 (9.9) |
| Wind Speed (m/s) | 13.5 (16.0) | 9.5 (16.1) | 6.6 (10.2) | 5.0 (7.7) |

583 *Measurements are given for the average with the maximum in the parenthesis.

Atmos. Chem. Phys. Discuss., doi:10.5194/acp-2016-1107, 2017
Manuscript under review for journal Atmos. Chem. Phys.
Published: 25 January 2017


Atmospheric Chemistry and Physics Discussions

584 **Figure Captions**

585

586 Figure 1. Temporal variations of measured species, including PAN, $PM_{10}$, $O_3$, $NO_2$, NO, $SO_2$,
587 and, CO, and meteorological parameters, including relative humidity, temperature,
588 and wind speed in fall 2010. Episodes 1–4, described in the main text, are shaded
589 in blue and yellow.

590 Figure 2. Diurnal variations in the concentrations of $O_3$, $NO_2$, PAN, and $PM_{10}$, measured at
591 GCO in the fall of 2010 (5 min data of $O_3$, $NO_2$, 2 min data of PAN, and 1 h data of
592 $PM_{10}$).

593 Figure 3. Comparison of $O_3$ with the PAN daily maxima. The time when the daily maximum
594 appears is classified as daytime (08–18 h) and nighttime (the rest) based on the
595 time of sunrise and sunset. Numerals indicate the days.

596 Figure 4. The three-day NOAA HYSPLIT backward trajectories of air masses for every one
597 hour observed at GCO during episode 1 (Oct. 31to Nov. 2), episode 2 (Oct. 28–29),
598 episode 3 (Oct. 20–21), and episode 4 (Nov. 4–5). They are colored according to
599 the level of (a) PAN, (b) $O_3$, and, (c) $NO_2$ at GCO at the time of the trajectory
600 initialization. The trajectories north of 50°N are not shown.

601 Figure 5. Correlations among PAN, $PM_{10}$, $O_3$, and carbonaceous compounds in $PM_{2.5}$: (a) $O_3$
602 and PAN, (b) $NO_2$ and PAN, and (c) $O_3$ and PAN. The red lines in (a) and (b)
603 represent linear regression for episode 4.

604 Figure 6. Correlations among PAN, $K^+$ ion of $PM_{1.0}$, and carbon components of $PM_{2.5}$ for
605 three cases: (a) $PM_{10}$ and PAN, (b) $PM_{2.5}$ OC and PAN, (c) $PM_{2.5}$ EC and PAN, (d)
606 $PM_{2.5}$ OC and EC, (e) $PM_{1.0}$ $K^+$ and PAN, and (f) $PM_{1.0}$ $K^+$ and $PM_{2.5}$ OC. The red
607 lines represent linear regression for episode 4.

608 Figure 7. Comparison between the observed and calculated (a) PAN and (b) $O_3$
609 concentrations by CAM-chem model.

610

Atmos. Chem. Phys. Discuss., doi:10.5194/acp-2016-1107, 2017
Manuscript under review for journal Atmos. Chem. Phys.
Published: 25 January 2017


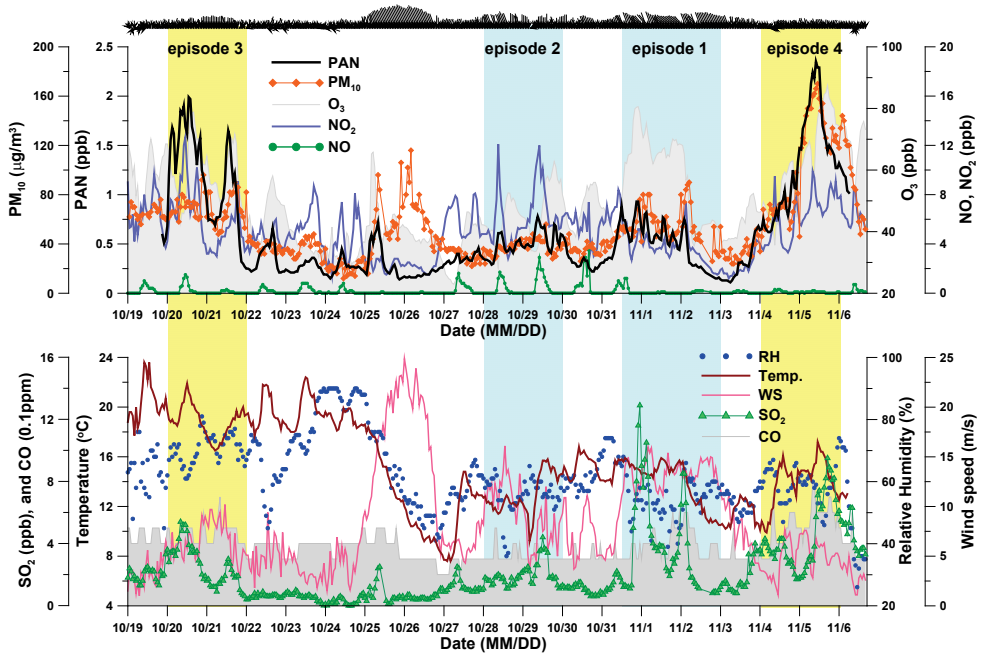


611
612

613 Figure 1.

Atmos. Chem. Phys. Discuss., doi:10.5194/acp-2016-1107, 2017
Manuscript under review for journal Atmos. Chem. Phys.
Published: 25 January 2017


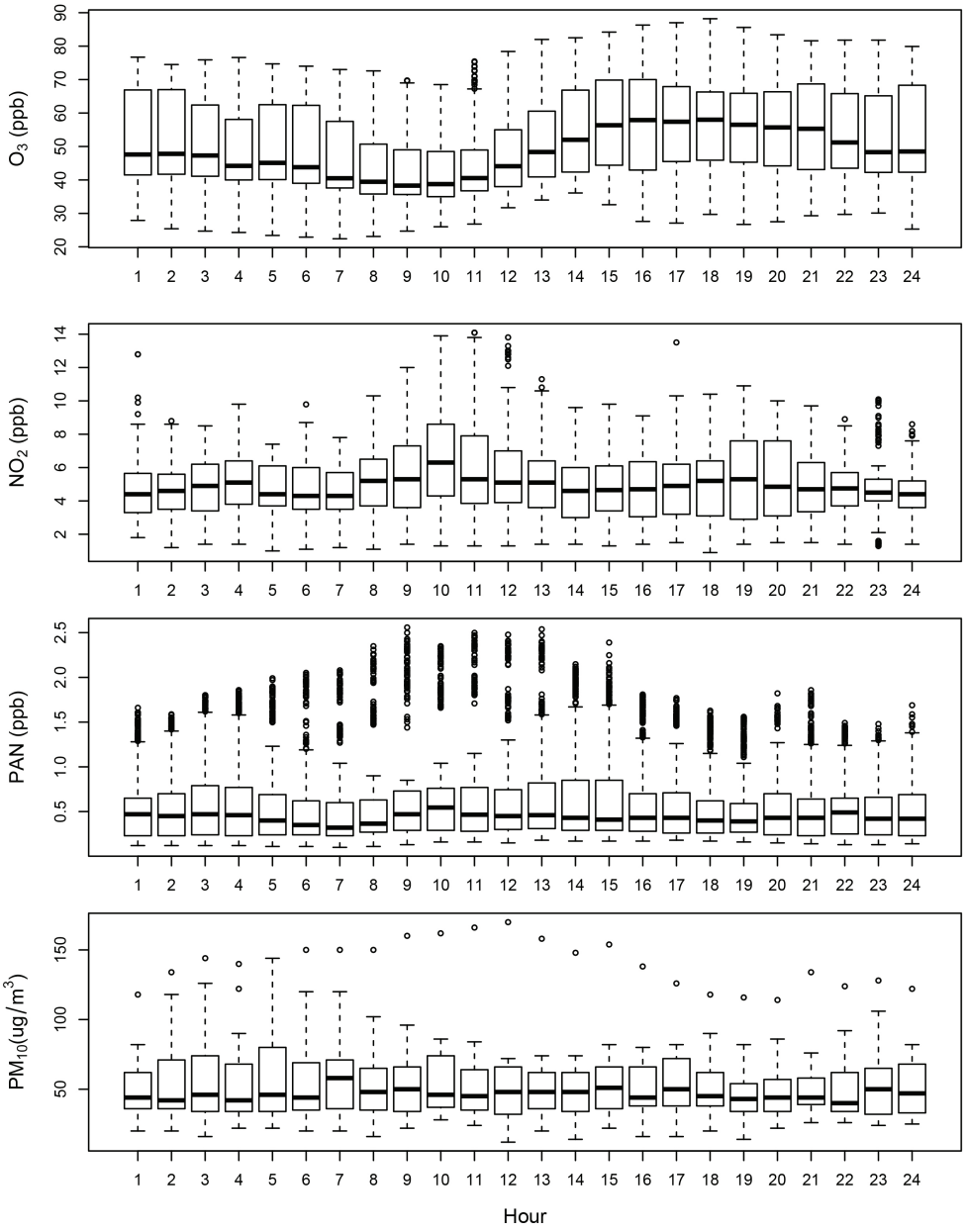


614

615 Figure 2.

Atmos. Chem. Phys. Discuss., doi:10.5194/acp-2016-1107, 2017
Manuscript under review for journal Atmos. Chem. Phys.
Published: 25 January 2017


Atmospheric Chemistry and Physics Discussions

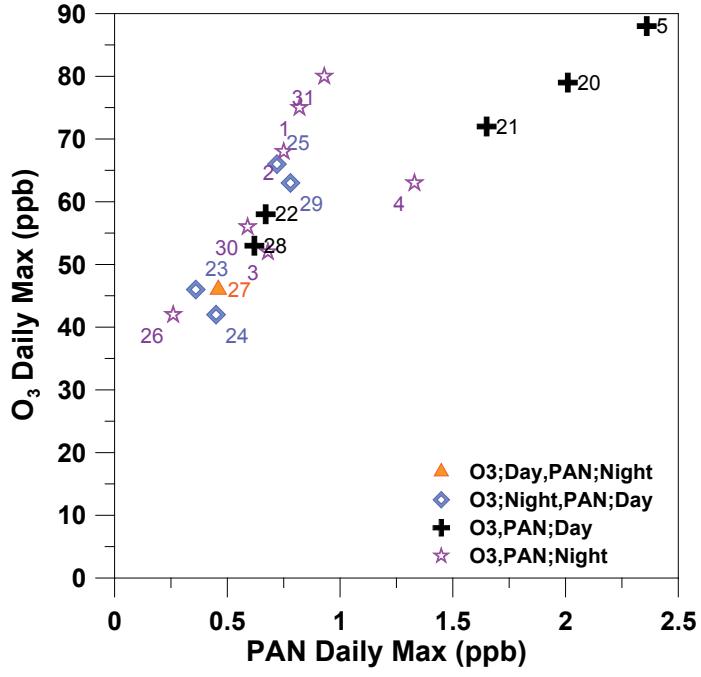


616

617 Figure 3.

Atmos. Chem. Phys. Discuss., doi:10.5194/acp-2016-1107, 2017
Manuscript under review for journal Atmos. Chem. Phys.
Published: 25 January 2017


Atmospheric Chemistry and Physics Discussions

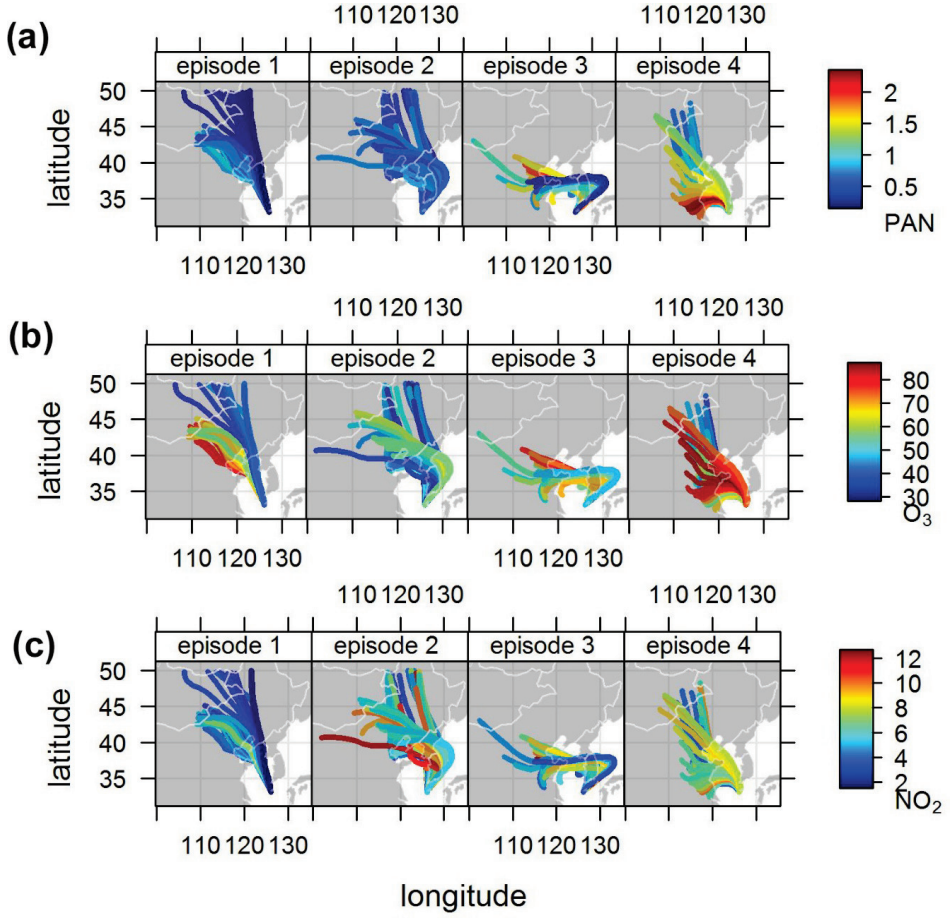


618

619 Figure 4.

Atmos. Chem. Phys. Discuss., doi:10.5194/acp-2016-1107, 2017
Manuscript under review for journal Atmos. Chem. Phys.
Published: 25 January 2017


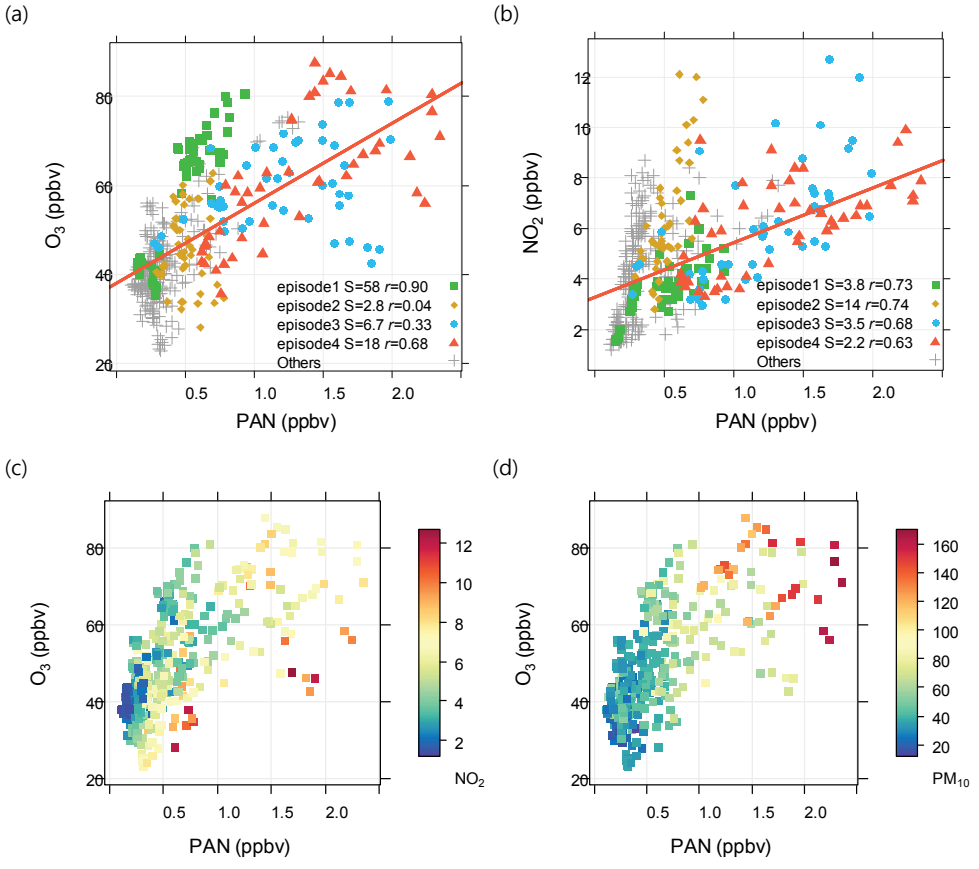


620

621 Figure 5.

Atmos. Chem. Phys. Discuss., doi:10.5194/acp-2016-1107, 2017
Manuscript under review for journal Atmos. Chem. Phys.
Published: 25 January 2017


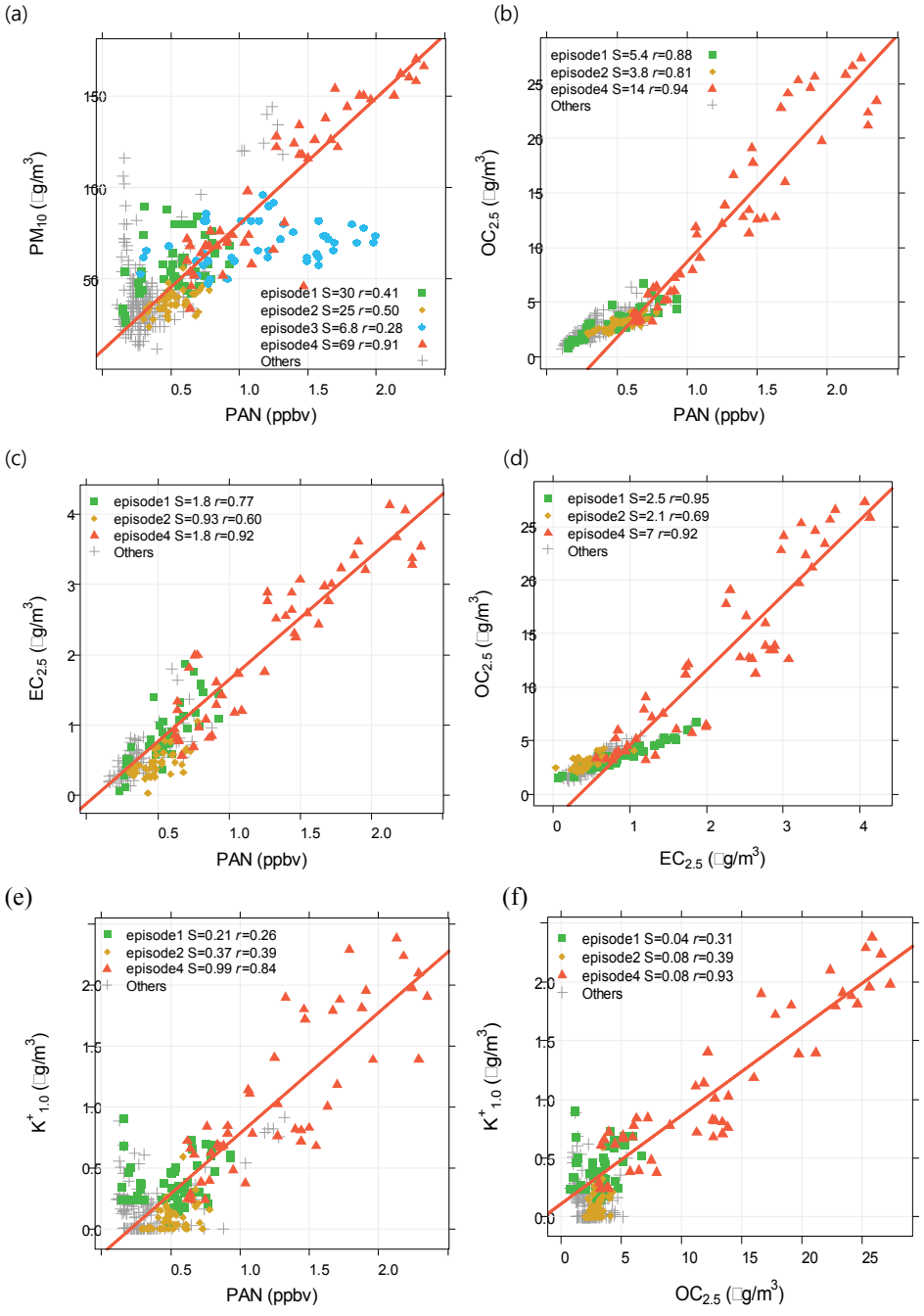


Figure 6.

Atmos. Chem. Phys. Discuss., doi:10.5194/acp-2016-1107, 2017
Manuscript under review for journal Atmos. Chem. Phys.
Published: 25 January 2017


Atmospheric Chemistry and Physics Discussions

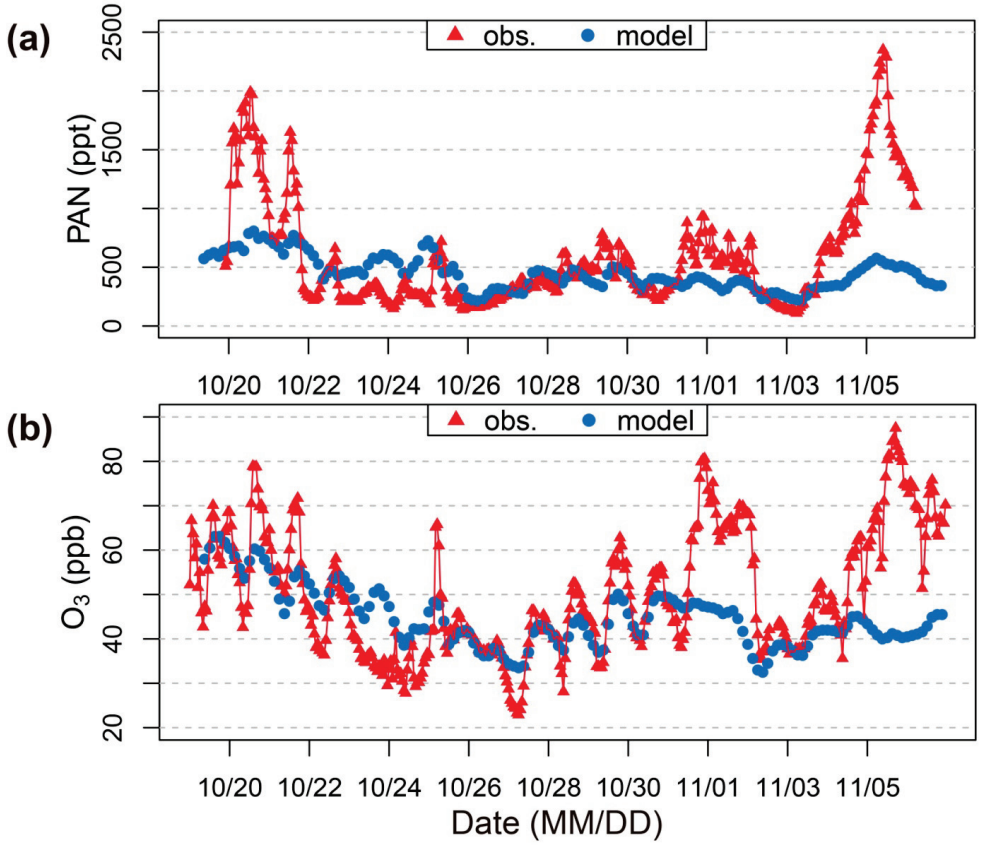


624

625 Figure 7.